INTERFACE STRESSES BETWEEN SOIL AND LARGE DIAMETER DRILLED SHAFT UNDER LATERAL LOADING

Kerop D. Janoyan[1], P.E., Member, Geo-Institute, and Matthew J. Whelan[2]

ABSTRACT: Results are presented of a field testing program for a full-scale, large diameter cast-in-drilled-hole (CIDH) shaft/column under large displacement cyclic lateral loading. The test shaft was extensively instrumented to enable high-precision section curvature measurements in addition to measurements of contact pressure at the soil-shaft interface around the shaft perimeter. Among the principal objectives of the testing was to characterize the soil-shaft interaction across a wide displacement range in order to gain insight into the adequacy of existing design guidelines (which are based principally on the testing of small diameter piles) for the large diameter shafts commonly used to support highway bridges. The component stresses of resistance and the effects of nonlinear soil resistance to relative displacements between the soil and shaft are presented.

INTRODUCTION

Pile-supported bridges provide an economical option for highway construction, particularly in seismic regions. The inelastic deformations for a pile/column under lateral loading occur below grade; therefore, the overall lateral load behavior of the system is influenced by the interaction between the shaft and the surrounding soil, commonly modeled using *p-y* curves. The prediction of soil-pile-structure system behavior under lateral loading is among the most complex topics in geotechnical

[1]Assistant Professor, Clarkson University, Department of Civil and Environmental Engineering, Potsdam, NY 13699
kerop@clarkson.edu
[2]Undergraduate Research Assistant, Clarkson University, Department of Civil and Environmental Engineering, Potsdam, NY 13699
whelanmj@clarkson.edu

engineering. Current models for *p-y* curves are calibrated primarily from lateral load testing of relatively small diameter piles. Since the soil resistance is such a critical consideration, there is a need for better understanding of its component stresses, particularly for large-diameter piles and drilled shafts.

The beam on nonlinear Winkler foundation (BNWF) model that gives rise to the use of *p-y* curves in engineering design is based upon the concept that soil-shaft interaction can be represented by a compressive force per unit length of shaft (McClelland and Focht 1958). As seen in Fig. 1, this force is the resultant of several stresses, including:

- Normal compressive stress on the leading face of the shaft, which in general will be some percentage of the passive soil capacity.
- Shear stress along the sides of the shaft.
- Active normal soil stresses on the trailing face of the shaft.

Current sensor technology only allows measurements of normal stress in soil, so interface shear stresses can only be indirectly inferred.

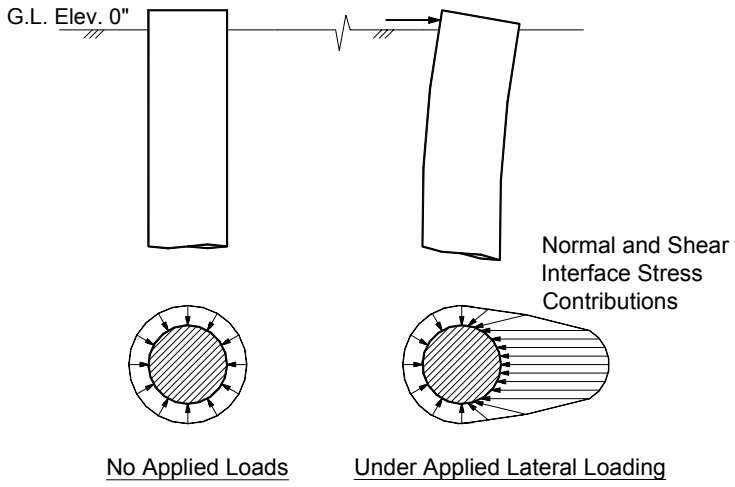

FIG. 1. Distribution of unit stresses against a pile before and after lateral displacement

This experimental study evaluated total soil reaction *p* from measurements of the internal bending deformation of the shaft through use of beam theory. The normal stresses at the soil-shaft interface, which were measured during field testing with non-displacement soil pressure cells (SPC), are compared to the total soil reaction and the interface shear stresses are calculated.

PREVIOUS STUDIES OF INTERFACE STRESSES

Few experimental studies of soil-shaft interface stresses have been performed because of difficulties associated with the use of SPCs. Such devices are obviously impractical for driven piles, but can be used in drilled shafts. The SPCs can be installed on the shaft wall after excavation of the shaft hole and placement of the

reinforcing cage, but prior to concrete placement. Such installations are only practical when the dry method of construction is used, i.e. no slurry. Among the previous studies of laterally loaded drilled shafts which have utilized soil pressure cells (Kasch et al. 1977 and Briaud et al. 1983, 1985), the work by Bierschwale et al. (1981) is of particular interest because the pressure cell data are well documented, and data for several azimuthal angles relative to the direction of loading are available.

The study consisted of lateral load testing of three separate reinforced concrete drilled shafts of varying diameters of roughly 0.9 m (2.5 ft) installed at a stiff clay site and laterally loaded at ground line. The SPCs were generally installed in the line of loading, and the results were plotted as a function of depth for various levels of head load. The authors did not evaluate distributions of p for comparison to pressure profiles. A simple equilibrium check was performed by assuming that the measured pressures were uniformly applied over the projected diameter of the shafts, and then summing the moments about the point of zero lateral stress. The results indicated a lack of equilibrium, and that a substantial increase of soil pressure near the top of the shaft would be required to achieve equilibrium. Lateral pressures off the line of loading were also measured and the results were presented. The result shows a significant reduction of normal stress 45 degrees from the line of loading at small load levels, but more nearly uniform stresses at higher load levels.

TEST SITE CONIDITIONS, SPECIMENT SETUP AND INSTRUMENTATION OF PRESENT STUDY

Site Conditions

The present study was conducted at the interchange of Interstate Highways 105 and 405 in Hawthorne, California, just southeast of the Los Angeles International Airport (Janoyan 2001). The mapped local geology is Quaternary alluvium. Field in-situ and laboratory testing was performed to characterize the soil conditions at the site. The field testing included seismic cone penetration testing (SCPT), rotary-wash borings with standard penetration testing (SPT), down-hole suspension logging of shear wave velocities, pressuremeter testing (PMT), and test pit excavation mapping. Samples for laboratory testing were retrieved from the borings using thin-walled Pitcher tubes, and were hand-carved from the walls of the test pit. Laboratory testing was performed to evaluate particle size distribution, Atterberg limits, shear strength, and consolidation characteristics.

A generalized soil profile for the site is presented in Fig. 2 and consists of:

- 0.6 to 1.5 m (0 – 2 to 5 ft): Fill consisting of asphalt and concrete debris.
- Formation 1 (base of fill – approximately 5.5 m to 7.3 m (18 to 24 ft)): Silty clay. Classification testing indicates moderate plasticity (PI ~ 15), approximately 60% fines. A silty sand interbed with a thickness of about 0.6 m (2 ft) occurs at a depth of approximately 3 m (10 ft) within this layer.
- Formation 2 (base of Formation 1, about 0.6 m to 1.2 m (2 to 4 ft) in thickness): Medium- to fine-grained silty sand/sandy silt. Classification testing indicates 30% fines and PI ~ 12. SPT blow counts are approximately 20 to 45.

- Formation 3 (base of Formation 2 – approximately 14.6 m (48 ft)): Silty clay. Classification testing indicates 40% fines and PI ~ 13 to 14.
- A medium sand underlies Formation 3, and is water bearing (i.e., the groundwater table is located within this layer).

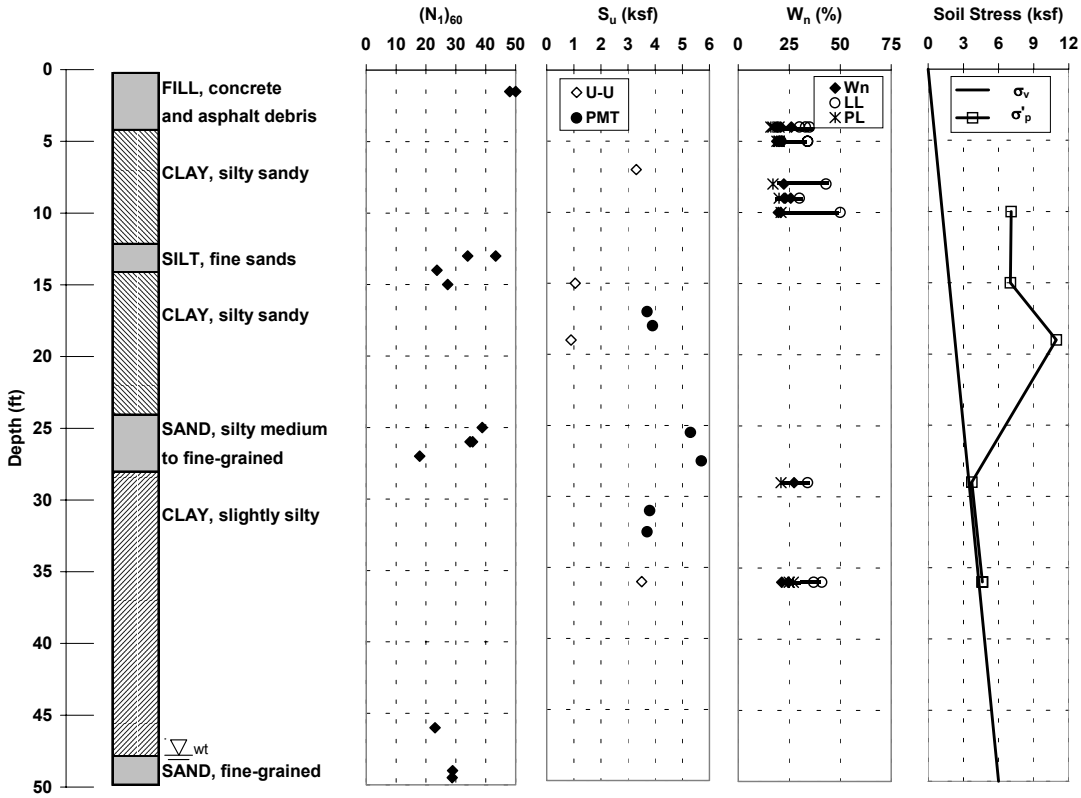

FIG. 2. Generalized test site soil profile along with some results from field and laboratory investigations

Specimen Setup

The CIDH shaft-column was designed according to standard Caltrans' Bridge Design Specifications (1995) using the Seismic Design Criteria (1999). The test specimen was comprised of a 1.8 m (6 ft) diameter column extending 12.2 m (40 ft) and a 2 m (6.5 ft) diameter shaft extending 14.6 m (48 ft) below ground line, as shown in Fig. 3. Steel reinforcement was comprised of 36-#14 longitudinal bars with average yield and ultimate tensile strengths of 490MPa (71 ksi) and 703 MPa (102 ksi), respectively; and shop-welded #8 hoops at 152 mm (6 inch) spacing with average yield and ultimate tensile strength of 496 MPa (72 ksi) and 738 MPa (107 ksi), respectively. The longitudinal and transverse steel ratios are roughly 2 per cent and 0.7 per cent, respectively. Normal-weight ready-mix concrete was used in the specimen, with an average tested cylinder compressive strength of 42 MPa (6.1 ksi).

Lateral loads were imposed at the top of the column using tension cables reacting against soil anchors at an angle of 26.6 degrees from the horizontal (2H:1V). Testing

of the shaft/column was displacement controlled. Cyclic lateral loading was applied across an amplitude range of 50 mm to 2.75 m (2 to 108 inches). Two loading cycles were performed at most displacement levels. Cycles at displacement amplitudes greater than 152 mm (6 inches) included 16 stops to enable measurements of the shape of hysteretic response curves.

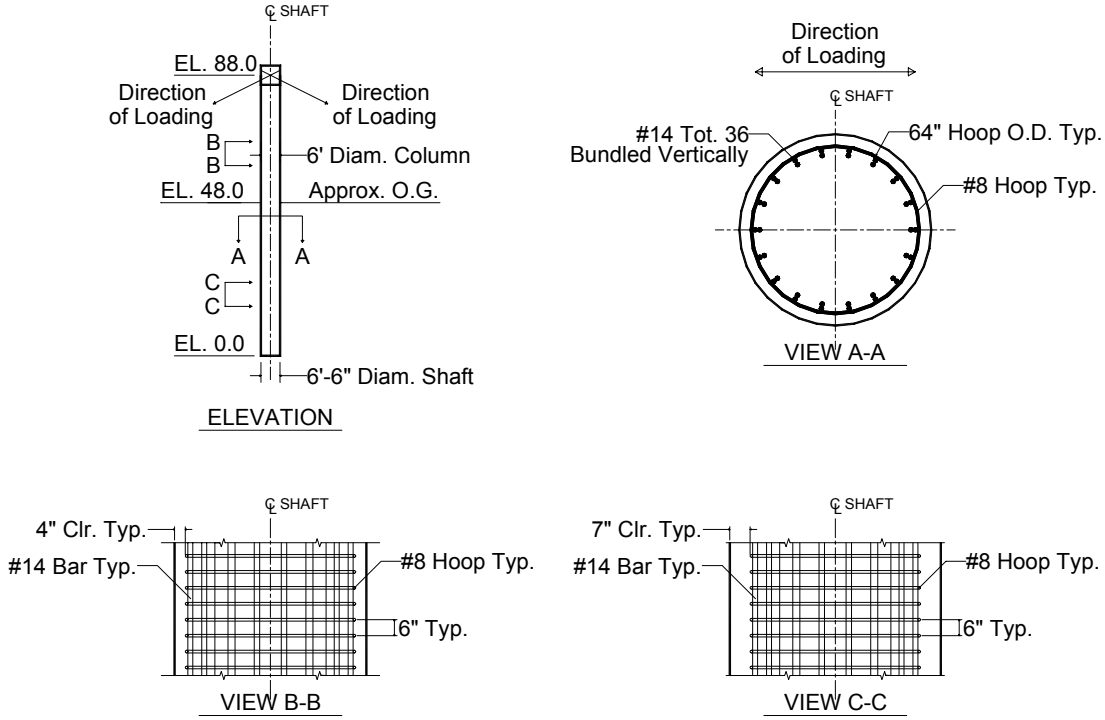

FIG. 3. Shaft/column section reinforcement details

Instrumentation

Extensive instrumentation, totaling over 200 channels of data, was used to monitor the response of the soil/shaft system and the local deformation of the column. Shaft bending deformations were measured with a redundant system of extensometers, inclinometers and high-precision fiber-optic sensors. The lateral displacement of the column (above ground) was measured using survey/total stations while the tilt at and below ground level shaft was measured using the inclinometers.

Profiles of soil reaction *p* and shaft displacement y were derived from the measured shaft curvature and displacement profiles, which were then used to generate *p-y* curves at various depths below ground. Janoyan (2001) and Janoyan et al. (2001) present details of the field measurements and data reduction techniques.

Other instrumentation included non-displacement soil pressure cells (i.e. cells with the approximate stiffness of concrete) which were installed at the interface between the concrete and soil. A total of 26 cells were installed at seven depths along the shaft both in the line of loading, and at several depths, at 30 and 60 degrees from the line of

loading (Fig. 4). Each cell was installed by hand on the excavation wall after the cage had been placed and immediately prior to concrete placement.

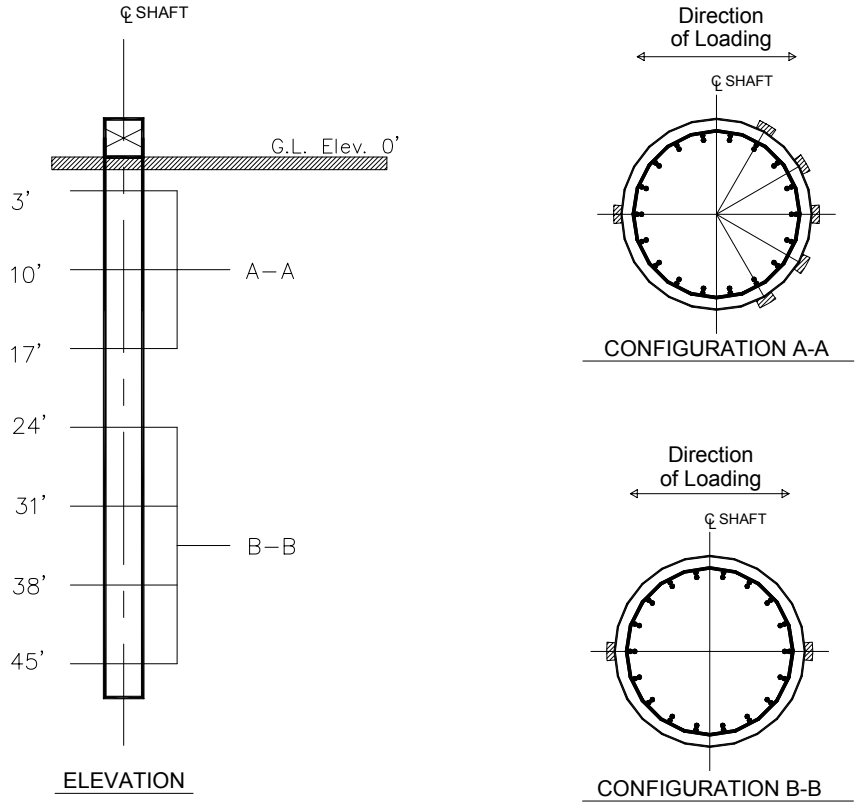

FIG. 4. Locations of soil pressure cells on test shaft

SOIL PRESSURE DISTRIBUTIONS FROM PRESENT TEST

Measured lateral soil pressures at the 22.9 cm (9 in) displacement level are plotted in Fig. 5 as a function of depth along with the lateral soil reaction profiles evaluated (from the analysis of *p*-*y* curves). The shapes of the profiles are comparable, and appear to have similar cross-over depths of about 3.7 m (12 ft). Similar plots were also generated at the other displacement levels.

Horizontal distributions of soil pressure around the shaft perimeter were measured at depths of 0.9 m (3 ft), 3.1 m (10 ft), and 5.2 m (17 ft). The horizontal distribution of pressures at the 0.9 m (3 ft) depth is shown in Fig. 6 for displacement levels up to 45.7 cm (18 in). As had been found in previous work (e.g., Bierschwale et al., 1981), normal soil stresses drop off significantly for azimuths off the line of loading. As seen in Fig. 6, the soil stresses along azimuths off the line of loading are not symmetric with respect to the loading direction. The lack of symmetry could have been due to some twisting of the reinforcing cage during placement; however the areas under the profiles are deemed to be reliable. Thus these readings were integrated around the shaft semi-perimeter to estimate the resultant normal stress acting against the shaft in the line of loading (p_σ),

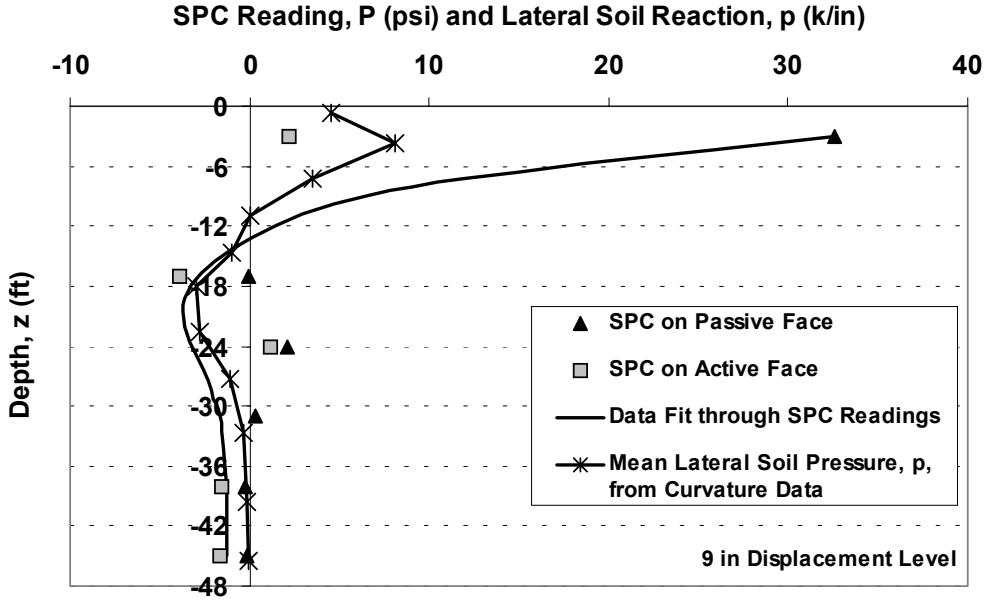

FIG. 5. Soil pressure cell reading, *P*, and soil reaction, *p*, distribution profiles for pull to west at 22.9 cm (9 inch) displacement level

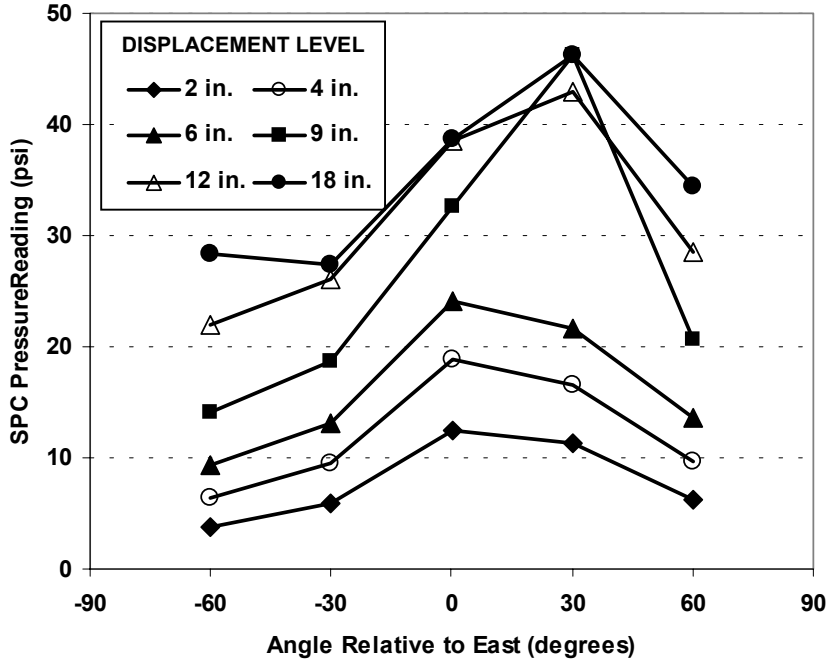

FIG. 6. Horizontal distribution of normal soil pressures against leading face of shaft at 0.9 m (3 ft) depth

$$p_\sigma = \int_{\theta=-\pi/2}^{\pi/2} \sigma(\theta)\cos\theta \cdot r \cdot d\theta \qquad (1)$$

where θ = azimuthal angle relative to line of loading. As noted earlier, the soil reaction against the shaft has contributions from passive soil resistance (i.e., the p_σ term), side shear resistance, and active pressures (which counteracts the resultant). As shown in Fig. 5, the active pressures are negligibly small. Hence, a good estimate of the side shear contribution (p_τ) can be obtained as the difference between p and p_σ.

To illustrate the effect of normal and side shear stresses on p at 0.9 m (3 ft) depth, the ratio of p_σ/p as a function of displacement level is plotted in Fig. 7. The results indicate that only about 20% of the soil reaction force p can be attributed to normal soil stress, and that this ratio does not vary with load level. Similar plots at the 3.1 m (10 ft) and 5.2 m (17 ft) depth levels (Fig. 7) reveal a different result, which is an increase of p_σ/p from about 15% to 25% at low displacement levels (i.e., displacements less than 22.9 cm or 9 in) to as high as 48% at the 45.7 cm (18 in) displacement level.

At all three depths, the modest contribution to p from p_σ is consistent with the previous results of Bierschwale et al. (1981) which found that substantial soil resistance beyond the normal stress was required to place the shaft in equilibrium. The trends at the 3.1 m (10 ft) and 5.2 m (17 ft) depths suggest that the side friction is mobilized early in the test and provides the majority of the resistance at low displacement levels. However, at larger displacements, the normal stresses account for an increasing fraction of p, suggesting a disproportionate build-up of p_σ with increasing shaft deflection.

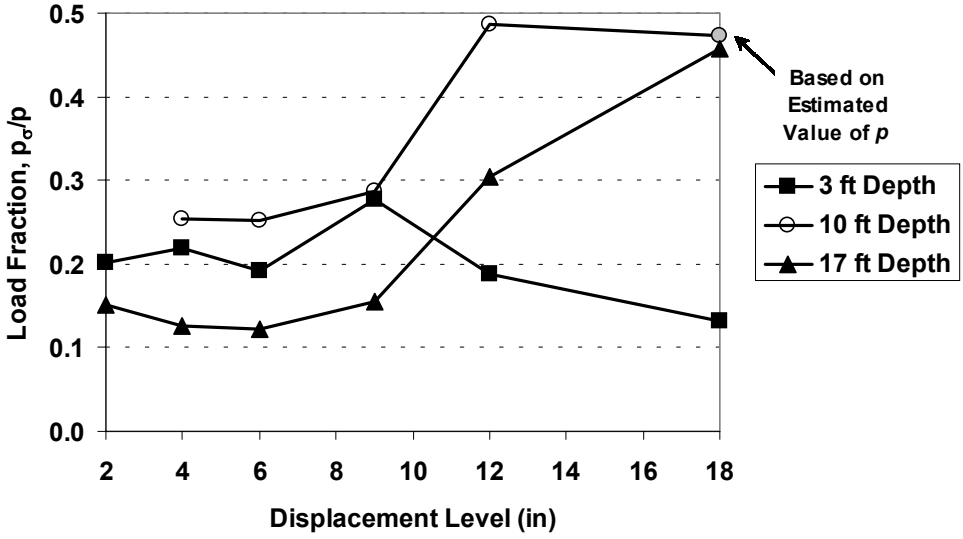

FIG. 7. Fraction of soil reaction force *p* that can be attributed to normal stresses at the soil-shaft interface as a function of displacement level at 0.9 m (3 ft) depth, 3.1 m (10 ft) depth, and 5.2 m (17 ft) depth

This observation is consistent with test results reported by Smith and Slyh (1986), who performed lateral load testing of a circular rigid concrete shaft, and found that side shear could account for 84% of the soil reaction at low displacement levels. Smith and Slyh (1986) provided a schematic illustration of this data trend, which is shown in Fig. 8.

The same trend is not apparent at the 0.9 m (3 ft) depth (Fig. 7). The soil reaction values, p, back-calculated in the p-y derivations increase nearly linearly with y. This increase essentially matches, on a percentage basis, the increase in cell pressures, which accounts for the uniform p_σ/p values shown at the 0.9m (3 ft) depth plot in Fig. 7. This result may not be reliable, however, because the p values at this depth were found to be unusually high (i.e., higher than the available soil resistance).

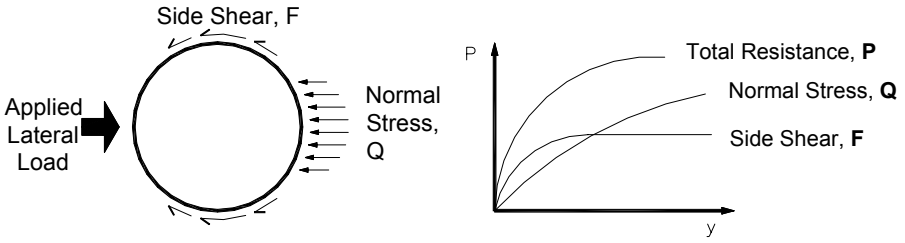

FIG. 8. The two components of soil resistance, *p* (after Smith and Slyh 1986)

CONCLUSIONS

In this study, p-y curves for a large diameter drilled shaft were directly inferred from field testing measurements through a carefully conceived data reduction program. Soil pressure cell data was then used to infer distributions of normal stress around the perimeter of the shaft at appropriate displacement levels. These pressure distributions were integrated around the shaft perimeter to evaluate the resultant soil reaction force per unit length at various depths. The results were used to evaluate the contribution of p_σ to p-values at each displacement level.

Insights into the mechanics of p-y response were obtained from the soil pressure cell data, which enabled the relative contributions of soil normal and shear stresses on p-values to be inferred. The relative contributions of normal stresses were seen to increase with shaft deflection, as passive pressures were mobilized on the face of the shaft. This study suggests that the side friction mobilized early in the test and provided the majority of the resistance at low displacement levels. However, at larger displacements, the normal stresses accounted for an increasing fraction of p, suggesting a disproportionate build-up of p_σ with increasing shaft deflection. Such behavior suggests that large diameter shafts could have added capacity from side friction, which the current design models do no incorporate.

ACKNOWLEDGMENT

Support for this research was in part provided by the California Department of Transportation (Caltrans) under Research Contract No. 59A0183 with contract

monitors Craig Whitten and Anoosh Shamsabadi at Caltrans and principal investigators John Wallace and Jonathan Stewart at the University of California, Los Angeles. Their support is gratefully acknowledged.

REFERENCES

Bierschwale, M., Coyle, H., and Bartoskewitz, R. (1981). "Lateral Load Tests on Drilled Shafts Founded in Clay," *Drilled Piers and Caissons*, ASCE, 98-113.

Briaud, J., Smith, T., and Meyer, B. (1983). "Pressuremeter Gives Elementary Model For Laterally Loaded Piles," *Intl. Symp. on In Situ Testing of Soil and Rock*, Paris.

Briaud, J., Smith, T., and Tucker, L. (1985). "A Pressuremeter Method for Laterally Loaded Piles," *Intl. Conf. Soil Mechanics and Foundation Engineering*, San Francisco.

California Department of Transportation (Caltrans). (1995). "Bridge Design Specifications Manual".

California Department of Transportation (Caltrans). (1999). "Caltrans Seismic Design Criteria".

Janoyan, K. (2001). "Interaction between Soil and Full-Scale Drilled Shaft under Cyclic Lateral Load." Ph.D. Dissertation, Dept. of Civil & Envir. Engrg., University of California, Los Angeles, CA.

Janoyan, K., Stewart, J. P., and Wallace, J. W. (2001). "Analysis of p-y Curves from Lateral Load Test of Large Diameter Drilled Shaft in Stiff Clay," *Proc., 6th Caltrans Workshop on Seismic Research*, Sacramento, CA, paper 5-105.

Kasch, V., Coyle, H., Bartoskewitz, R., and Sarver, W. (1977). "Lateral Load Test of a Drilled Shaft in Clay," *Research Report No. 211-1*, Texas Transportation Institute, Texas A&M University, College Station.

McClelland, B. and Focht, J. (1958). "Soil Modulus for Laterally Loaded Piles," *Transactions,* ASCE, Vol. 123, Paper 2954, 1049-1086.

Smith, T. and Slyh, R. (1986). "Side Friction Mobilization Rates for Laterally Loaded Piles from the Pressuremeter," *The Pressuremeter and Its Marine Applications: Second Intl. Symposium*, ASTM STP 950, 478-491.

APPENDIX I. CONVERSION TO SI UNITS

Inches (in) × 0.0254 = meter (m)
Feet (ft) × 0.3048 = meter (m)
Kips per square foot (ksf) × 47.88 = kilopascals (kPa)
Kips per square inch (ksi) × 6.894 = Megapascals (MPa)
Pounds per square inch (psi) × 6.894 = kilopascals (kPa)
Kips per inch (k/in) × 175.1 = kinonewton per meter (kN/m)